A98-31619

ICAS-98-4,11,2

OPTIMAL PLACEMENT OF PIEZOELECTRIC SENSORS AND ACTUATORS USING COMBINATORIAL OPTIMIZATION

L. Cardascia[1], R. Ruotolo[2], G. Surace[2]
[1] Dept. of Structural Engineering
[2] Dept. of Aeronautical and Space Engineering
Politecnico di Torino - ITALY

Abstract

The purpose of this paper is to optimize the placement of n pairs of piezoelectric sensors and actuators with a view to reducing vibration of a composite beam. Using the Reissner-Mindlin model to describe beam behaviour, both sensor and actuator are considered as layers of composite material. The position and length of each sensor-actuator pair is determined by applying genetic algorithms to maximize a function including the product of damping ratio by natural frequency in each mode. Some numerical simulations, which through comparison with experimental results show the importance of an accurate damping model due to the layer of adhesive and to piezoelectric patches, complete the work.

Introduction

Intelligent structures have received considerable attention in recent years. Through a highly distributed network of sensors and actuators, such structures allow the control of effects produced by an external disturbance by applying appropriate forces. As the number of these actuators in an intelligent structure is quite high, it is desirable that they be compact and lightweight. In addition, they should cause no substantial change in the static and dynamic behaviour of the structure to which they are coupled. Piezoelectric materials can be used for this purpose.

Control of flexible structures as undertaken by Crawley [1] and Bailey and Hubbard [2] is based on the potential of piezoelectric actuators for inducing structural deformation. It is evident that the success of the control is related to the position of the sensors and actuators [3]. A number of investigations have tackled the problem of determining optimum placement and size of piezoelectric patches so as to minimize the amount of control [4], whilst others have solved the problem by considering the grammian of controllability or closed-loop eigenvalues [5].

As an alternative to classic optimization techniques, which have the drawback of stopping short of local optimum points, advanced techniques such as genetic algorithms [6] and simulated annealing [7] have emerged lately. In [8] genetic algorithms are used for placement and determination of optimum piezoelectric patch size considering amplitude of the desired mode as target function.

The majority of works on both beams and plates use simplified models based on Kirchhof's assumptions. This paper describes structural behaviour using a mathematical model which, taking into account also shear deformation, equally applies to structures whose thickness is not negligible relative to the other dimensions. Moreover, the mathematical model also includes damping due to both adhesive layer and piezoelectric patch.

The aim is to determine the optimum placement and size of piezoelectric patches placed on a composite beam. The structure has been discretized using the finite element method, whereas genetic algorithms were used for placement and sizing of piezoelectric patches so as to obtain maximum attenuation of vibration on the structure. Numerical examples are used to show the effect of considering a target function incorporating both the product of damping ratio times natural frequency and the angle of fiber orientation of the composite material.

Mathematical model

To determine the dynamic response of a composite plate with actuator and sensor inside the structure or glued to the surface, a calculation program was written on the basis of the procedure described in [9]. What follows is a brief outline of the main steps for producing a mechanical and electrical model of the plate with attached piezoelectrics.

Equations for the structural model

The displacement model used is that of the Reissner-Mindlin theory which considers both flexural and shear deformations. Displacement (u, v, w) of a coordinate point (x, y, z) is given by:

$$u(x, y, z) = u^0(x, y) + z\phi_{xz},$$

$$\begin{aligned} v(x,y,z) &= v^0(x,y) + z\phi_{yz}, \\ w(x,y,z) &= w^0(x,y), \end{aligned} \quad (1)$$

where u^0, v^0 and w^0 are the displacements of a point on the reference surface of the plate, whereas ϕ_{xz} and ϕ_{yz} represent rotations normal to the reference surface obtained by superimposition of rotations φ_{xz} and φ_{yz} due to deflection only and to rotations $w^0_{,x}$ and $w^0_{,y}$ due to shear:

$$\begin{aligned} \phi_{xz} &= \varphi_{xz} - w^0_{,x}, \\ \phi_{yz} &= \varphi_{yz} - w^0_{,y}. \end{aligned} \quad (2)$$

The stress-strain equation is obtained assuming kth layer to be homogeneous, orthotropous and linearly elastic. With fiber orientation of kth layer rotated through angle θ relative to x axis of global reference system, state equations become [9] [10]:

$$\begin{aligned} \left\{ \begin{array}{c} \sigma^p_\theta \\ \sigma^n_\theta \end{array} \right\}_k &= [C_\theta]_k \left\{ \begin{array}{c} \epsilon^p_\theta \\ \epsilon^n_\theta \end{array} \right\}_k \\ [C_\theta]_k &= [T_\theta][\bar{C}]_k[T_\theta]^T \end{aligned} \quad (3)$$

with

$$[\bar{C}]_k = \left[\begin{array}{cc} [\bar{C}_{pp}]_k & [\bar{C}_{pn}]_k \\ [\bar{C}_{np}]_k & [\bar{C}_{nn}]_k \end{array} \right]$$

$$[T_\theta] = \left[\begin{array}{ccccc} m^2 & n^2 & -2mn & 0 & 0 \\ n^2 & m^2 & 2mn & 0 & 0 \\ mn & -mn & m^2-n^2 & 0 & 0 \\ 0 & 0 & 0 & m & n \\ 0 & 0 & 0 & -n & m \end{array} \right] \quad (4)$$

$$m = cos(\theta) \qquad n = sin(\theta)$$

$$\begin{aligned} \{\sigma^p\}^T_k &= \{\sigma^k_{11}, \sigma^k_{22}, \sigma^k_{12}\} \\ \{\sigma^n\}^T_k &= \{\sigma^k_{23}, \sigma^k_{13}\} \end{aligned} \quad (5)$$

$$[\bar{C}_{pp}]_k = \left[\begin{array}{ccc} \bar{C}_{11} & \bar{C}_{12} & \bar{C}_{16} \\ \bar{C}_{12} & \bar{C}_{22} & \bar{C}_{66} \\ \bar{C}_{16} & \bar{C}_{26} & \bar{C}_{66} \end{array} \right]_k$$

$$[\bar{C}_{nn}]_k = \left[\begin{array}{cc} \bar{C}_{44} & \bar{C}_{45} \\ \bar{C}_{45} & \bar{C}_{55} \end{array} \right]_k \quad (6)$$

The deformations-displacements relationship makes use of von Kàrmàn's approximation [9]:

$$\begin{aligned} \{\epsilon^p\} &= \{\epsilon^p_l\} + \{\epsilon^p_{nl}\} = ([B^p_l] + [B^p_{nl}])\{u\} \\ \{\epsilon^n\} &= [B^n]\{u\} \\ \delta\{\epsilon^p\} &= \delta\{\epsilon^p_l\} + \delta\{\epsilon^p_l\} = ([B^p_l] + 2[B^p_{nl}])\delta\{u\} \\ \delta\{\epsilon^n\} &= [B^n]\delta\{u\} \end{aligned} \quad (7)$$

$$\{u\}^T = \{u_1, u_2, u_3\}$$

$$\begin{aligned} \{\epsilon^p\}^T &= \{\epsilon_{11}, \epsilon_{22}, \epsilon_{12}\} \\ \{\epsilon^n\}^T &= \{\epsilon_{13}, \epsilon_{23}\} \end{aligned} \quad (8)$$

$$\begin{aligned} [B^p_l] &= \left[\begin{array}{ccc} \partial_x & 0 & 0 \\ 0 & \partial_y & 0 \\ \partial_y & \partial_x & 0 \end{array} \right] \\ [B^n] &= \left[\begin{array}{ccc} \partial_z & 0 & \partial_x \\ 0 & \partial_z & \partial_y \end{array} \right] \end{aligned} \quad (9)$$

Electromechanical coupling equations

In order to use a piezoelectric material as sensor or actuator it is possible to take advantage of two types of effects. The first, known as converse effect, associates the stress imposed on a piezoelectric material with mechanical loads and strains according to the following relationship:

$$\{\sigma\}_k = [C]_k(\{\epsilon\}_k - [\mathcal{D}]_k\{\mathcal{E}\}_k) \quad (10)$$

where $[C]$ is the matrix of Hooke's law and $[\mathcal{D}]$ is the matrix of piezoelectric deformation coefficients:

$$[\mathcal{D}]^T_k = \left[\begin{array}{ccccc} 0 & 0 & 0 & 0 & \mathcal{D}_{15} \\ 0 & 0 & 0 & \mathcal{D}_{14} & 0 \\ \mathcal{D}_{31} & \mathcal{D}_{32} & \mathcal{D}_{36} & 0 & 0 \end{array} \right]_k$$

whereas the electric field vector is:

$$\{\mathcal{E}\}_k = \{\mathcal{E}_1, \mathcal{E}_2, \mathcal{E}_3\}_k = \{0, 0, -\mathcal{U}_{k,s}\}_k \quad (11)$$

The second type, known as the direct piezoelectric effect, where mechanical loading applied to a piezoelectric component generates electric charges or induced stress $\{\mathcal{S}_k\}$:

$$\{\mathcal{S}_k\} = [\mathcal{Z}_k]\{\mathcal{E}_k\} + [\mathcal{D}]^T_k\{\sigma\}_k \quad (12)$$

where the permissivity matrix is assumed to be diagonal:

$$[\mathcal{Z}]_k = diagonal\{\mathcal{Z}_{11}, \mathcal{Z}_{22}, \mathcal{Z}_{33}\}$$

Electric field model

Electric field is expressed at individual layer level and is assumed to feature a linear distribution along the layer. Therefore a quadratic stress is considered, as shown in Fig. 1, and of type [9]:

$$\begin{aligned} \mathcal{U}_k(x,y,z) &= f_t(\zeta_k)\,\mathcal{U}^t_k(x,y) + f_c(\zeta_k)\,\mathcal{U}^c_k(x,y) + \\ &\quad f_b(\zeta_k)\,\mathcal{U}^b_k(x,y) \\ \mathcal{U}_k &= \{E_\mathcal{U}\}^T_k\{X^k_\mathcal{U}\} \end{aligned} \quad (13)$$

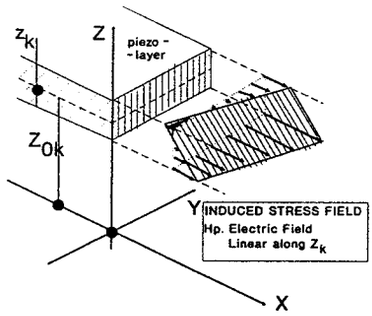

Figure 1: Induced stress by linear variation along z of the electric field in the piezo-layer

where $\mathcal{U}_k^t$, $\mathcal{U}_k^c$ and $\mathcal{U}_k^b$ represent stress at top, center and bottom of the layer. Interpolation functions are given in [9].

Displacement equation for laminated plate

For a multilayered plate of volume V subjected to mechanical and electrical loading by piezoelectric actuators, the principle of virtual works becomes:

$$\int_V (\{\delta\epsilon\}_k^T\{\sigma\}_k + \{\delta\mathcal{E}\}_k^T\{\mathcal{S}\}_k)dV = \delta L_e + \delta L_{in} \quad (14)$$

where $\int_V \{\epsilon\}_k^T\{\sigma\}_k dV$ is the part of virtual work due to mechanical deformation and to the stresses generated by the converse effect in the piezo-layer, $\int_V \{\delta\mathcal{E}\}_k^T\{\mathcal{S}\}_k dV$ is the part of virtual work due to the electric field in the piezo-layer through direct effect, $\delta L_e = \int_V \{\delta u\}_k^T\{P\}_k dV$ is the virtual work due to external mechanical loading $\{P\}$ and $\delta L_{in} = -\int_V \rho_k\{\delta u\}_k^T\{\ddot{u}\}_k dV$ is the virtual work due to inertia forces.

Finite element discretization

By substituting equations (1), (2), (3), (7), (10) and (12) in (14) we obtain an equation which will depend on variables $\{X_\mathcal{U}\}$ and $\{X_u\}$, which are the vectors of electrical and mechanical degrees of freedom of the structure respectively. If the structure is discretized in finite elements, the displacement vector may be expressed as a function of the vector for the degrees of freedom of the modes [11]:

$$\{X_u\} = [N_u]\{Q_u\}; \quad \{X_\mathcal{U}\}_k = [N_\mathcal{U}]\{Q_\mathcal{U}\}_k \quad (15)$$

where $[N_u]$ and $[N_\mathcal{U}]$ are matrices whose elements are the shape functions for mechanical and electrical displacements respectively. After discretization, equation (14) becomes:

$$\{\delta Q_u\}^T[K_{mm}]\{Q_u\} + \{\delta Q_u\}^T[K_{me}]\{Q_\mathcal{U}\}_k +$$

	Bottom surface at ground	Upper surface at ground
Actuator layer	$\mathcal{U}_b^k = 0$	$\mathcal{U}_b^k$ fixed
	$\mathcal{U}_c^k$ free	$\mathcal{U}_c^k$ free
	$\mathcal{U}_t^k$ fixed	$\mathcal{U}_t^k = 0$
Sensor layer	$\mathcal{U}_b^k = 0$	$\mathcal{U}_b^k$ free
	$\mathcal{U}_c^k$ free	$\mathcal{U}_b^k$ free
	$\mathcal{U}_t^k$ free	$\mathcal{U}_t^k = 0$

Table 1: Electrical boundary condition.

$$\{\delta Q_\mathcal{U}\}_k^T[K_{em}]\{Q_u\} + \{\delta Q_\mathcal{U}\}_k^T[K_{ee}]\{Q_\mathcal{U}\}_k = -\{\delta Q_u\}^T[M]\{\ddot{Q}_u\} + \{\delta Q_u\}^T\{P_m\} \quad (16)$$

where the mass matrices are those given in [9]. Stiffness matrices and mechanical-electric coupling matrices for piezo-layers of sensor and actuator are obtained by applying electrical boundary conditions as given in Table 1.

The displacement equations for a multilayered plate with piezo-layers as actuators and sensors, take up the following coupled shape [9]:

$$\begin{aligned}[K_{mm}]\{Q_u\} + [K_{me}]\{Q_\mathcal{U}\} + [M]\{\ddot{Q}_u\} &= \{P_m\} + \{P_{me}^A\} \\ [K_{em}]\{Q_u\} + [K_{ee}]\{Q_\mathcal{U}\} &= \{P_{ee}^A\} \end{aligned} \quad (17)$$

If we suppress the vector for electrical degrees of freedom $\{Q_\mathcal{U}\}$, the resulting equations are formulated in terms of displacement $\{Q_u\}$:

$$[K]\{Q_u\} + [M]\{\ddot{Q}_u\} = \{P_m\} + \{P_e\} \quad (18)$$

where

$$\begin{aligned}[K] &= [K_{mm}] - [K_{me}][K_{ee}]^{-1}[K_{em}] \\ \{P_e\} &= \{P_{me}^A\} - [K_{me}][K_{ee}]^{-1}\{P_{ee}^A\} \end{aligned} \quad (19)$$

Equations (19) demonstrate that piezoelectric patches modify stiffness matrices and external load inputs. The equation derived from (17),

$$\{Q_\mathcal{U}\} = [K_{ee}]^{-1}\{P_{ee}^A\} - [K_{ee}]^{-1}[K_{em}]\{Q_u\} \quad (20)$$

permits post-processing calculation of stresses generated at sensors' terminals.

Modal damping of the plate

The analysis of composite plate damping is carried out using the specific damping capacity (SDC) concept outlined in [10]:

$$\varphi = \frac{\Delta U}{U} = \frac{\{Q_u\}^T[K_d]\{Q_u\}}{\{Q_u\}^T[K]\{Q_u\}} \quad (21)$$

where ΔU is the energy dissipated during a stress cycle, U is the maximum deformation energy during a stress

cycle [10], $[K]$ is the stiffness matrix given in (19), $[K_d]$ is the 'damped' stiffness matrix [10] [12] given by:

$$[K_d] = \int_V [B]^T [\bar{C}_\theta^d][B] dV \tag{22}$$

The damping factor for the ith mode, of which $\{\phi_i\}$ is its modeshape, may be obtained as:

$$2\xi_i = \frac{1}{2\pi} \frac{\{\phi_i\}^T [K_d] \{\phi_i\}}{\{\phi_i\}^T [K] \{\phi_i\}} \tag{23}$$

The damping values thus calculated are introduced in the mode formulation of the displacement equation:

$$[\bar{M}]\{\ddot{\eta}\} + [\bar{C}]\{\dot{\eta}\} + [\bar{K}]\{\eta\} = \{\bar{F}\} \tag{24}$$

obtained from (18) following conversion to modal coordinates:

$$\{Q_u(t)\} = [\Phi]\{\eta(t)\} \tag{25}$$

Converting equation (24) to state space form we can write:

$$\begin{cases} \{\dot{x}\} = [A]_{ol}\{x\} + [B]_{ol}\{u_c\} \\ \{y\} = [C]_{ol}\{x\} + [D]_{ol}\{u_c\} \end{cases} \tag{26}$$

where

$$\begin{aligned} \{x\} &= \begin{Bmatrix} \{\eta\} \\ \{\dot{\eta}\} \end{Bmatrix} \\ [A]_{ol} &= \begin{bmatrix} 0 & [I] \\ -[\bar{M}]^{-1}[\bar{K}] & -[\bar{M}]^{-1}[\bar{C}] \end{bmatrix} \\ [B]_{ol} &= \begin{bmatrix} 0 \\ [\bar{M}]^{-1}[\bar{F}] \end{bmatrix} \\ \{y\} &= \begin{Bmatrix} \{\eta\} \\ \{\dot{\eta}\} \end{Bmatrix} \end{aligned} \tag{27}$$

Control input $\{u_c\}$ with constant feedback gain:

$$\{u_c\} = -G\,\{y\} \tag{28}$$

permits, for vibration control purposes, an increase in structure damping using piezoelectric sensors and actuators located as shown in Fig. 2, through feedback at $\{\dot{\eta}\}$.

Application of genetic algorithms

Genetic algorithms are optimization techniques derived from the natural selection process and from the evolution theory originally studied by Charles Darwin.

The evolution theory is applied, for function optimization, by associating first of all the concept of individual with a potential solution of the function to be optimized, and secondly by assessing the extent to which the individual adapts to the environment using the value of the target function $f(\cdot)$.

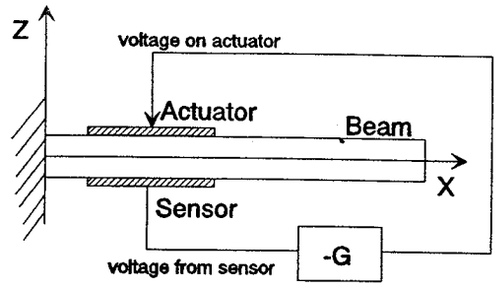

Figure 2: Beam with piezoelectric sensor and/or actuator

Thus, thanks to current calculation capability which permits evaluating very quickly the 'performance' of many individuals, i.e. calculating the value of the target function for a given array of potential solutions, we may apply the theory of the survival of the fittest individual of the population in question. The fittest will be the one who best adapts to the environment, and therefore whose target function is at a maximum.

To reach the optimum value for the problem under consideration, genetic algorithms were developed so as to proceed during optimization in a way similar to the natural evolution of the species - including the fundamental concepts of reproduction through exchange of chromosomes, random mutation of genes and natural selection.

In order to apply the theory of Darwin to an optimization procedure, the initial population chosen at random evolves over several generations producing new individuals better adapted to the environment. The degree of adaptation is assessed through the target function formulated on the basis of the specific optimization problem in hand. Moreover, depending on how reproduction, selection and mutation occur, based as they are on the draw of numbers at random, optimization techniques deriving from genetic algorithms are such that to stop the optimization process when a local maximum is reached.

When an initial population has been established, the next step is reproduction. The suitability of each individual to be chosen as 'parent' for the purpose of generating the next population is assessed by means of the target function, after applying selection criteria biased towards the probability of hitting on individuals with the highest degree of adaptability.

In natural evolution, genetic characteristics of offspring are derived from those of both parents. With genetic algorithms the crossover process ensures that genetic features of parents are passed on to their offspring. This occurs essentially by breaking and exchanging the genetic information of the two parents, so that two individuals generate two offspring. Thus, population size remains unchanged and becomes a spe-

cific parameter of the optimization procedure.

To prevent the entire population from converging towards local solutions of the optimization problem, it is introduced the concept of mutation which brings about the random variation of some genetic information on individuals within the population.

The intelligent structure design was optimized as regards the position and size of pairs of piezoelectric sensors and actuators using genetic algorithms. Composite fiber orientation was added as an added problem variable.

Placement and size optimization for n pairs of piezoelectric patches on the beam considered using genetic algorithms, was performed through random generation of n placement-size pairs, representing the generic individual to which the optimization procedure is aimed. Based on positions and sizes thus generated, each time a mesh must be rebuilt for structure discretization, also applying the procedure outlined in the previous section to assess damping and stiffness values.

Taking into account the significance of damping for vibration control - the higher the damping the better the closed loop system performance and the lower the need for control - we have used a target function to be maximized corresponding to the damping of the system illustrated in Fig. 2. Given the contribution of each mode, for the ith individual it was assumed:

$$f(\{p_x\}_i, \{l_x\}_i) = \sum_{j=1}^{N} 2c_j \xi_{j,i} \omega_{j,i} \qquad (29)$$

where c_j is the weight factor for each mode, $\{p_x\}_i$ and $\{l_x\}_i$ refer to centerline position and length of each sensor-actuator pair respectively.

Numerical results

To validate the mathematical model, we evaluated the static deflection of a bimorph beam as shown in Fig. 3. A comparison between results obtained with our model and those from the literature [12] [13] is illustrated in Fig. 4. Evidence confirms results are in good agreement.

Subsequent numerical examples concern a carbon-epoxy cantilever laminated composite beam and piezoceramic sensors and actuators in stacking sequence

$$[\theta_4/0_2/90_2]_s$$

. Initially, we assume θ equal to 0^o, 15^o, 30^o, 45^o, 60^o, 75^o, 90^o, beam size being $230 \times 20 \times 2$ mm^3, and piezoceramics $50 \times 20 \times 0.5$ mm^3. Mechanical properties of beam, piezoelectric ceramics and adhesive layer can be found in [14].

In Figures 5 and 6 damping ratio and damping term $2\xi\omega$ of composite beam of characteristics as mentioned

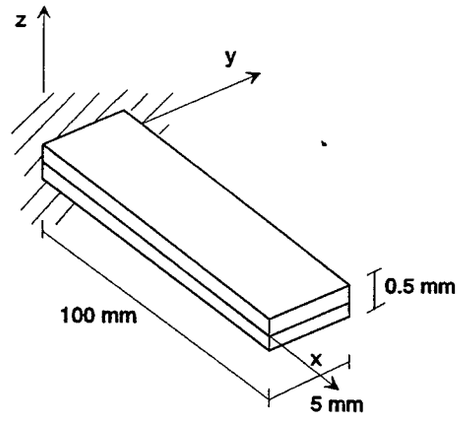

Figure 3: Piezoelectric polymeric PVDF bimorph beam

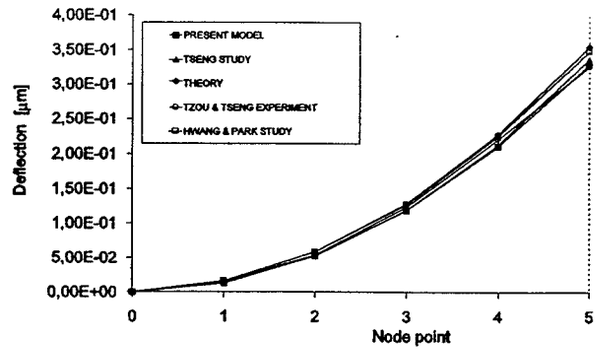

Figure 4: Deflection of the piezoelectric PVDF bimorph beam with input voltage of 1 V

previously and obtained with this matematical model, are compared with those obtained by experimental tests [14]. The above diagrams confirm the correctness of the mathematical model adopted herein, even with changing fiber orientation. Moreover, the figures also include the term 'present model *' with both adhesive layers and piezoceramics which are not considered by the mathematical model. Results indicate that damping by adhesive layer and piezoelectric sensors and actuators plays an important role in the dynamics of the system as a whole and must be taken into account during system modelling.

Simulations of optimum placement using the genetic algorithm were carried out on the same composite beam used for the previous example, including damping of both the adhesive layer and the piezoelectric patch, 5 pairs of piezoelectric sensors and actuators, with the condition that minimum size should not be under 0.01 m. A number of simulations were meant to determine optimum sensor and actuator placement and size considering first the damping of the first five modes separately. Subsequently, several other modes were considered to establish optimum placements for a structure

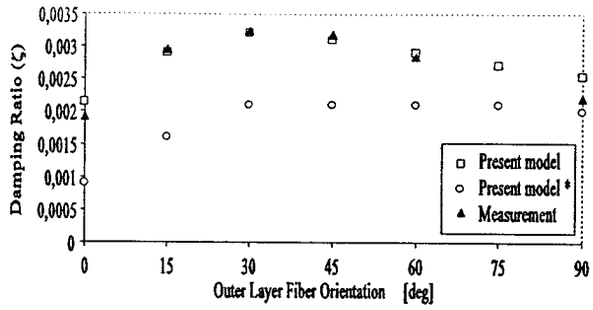

Figure 5: Damping for a composite beam, prediction and measurement

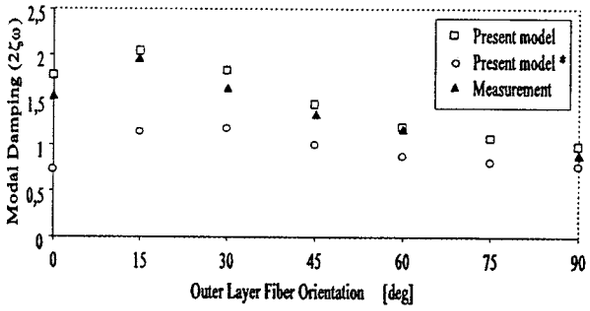

Figure 6: Damping for a composite beam, prediction and measurement

stressed in a wider frequency range.

Results obtained for each individual mode are summarized in Table 2 which shows position $p_{x,i}$ as the distance of average point of ith piezoelectric patch from the point of restraint, and in Table 3 which shows length $l_{x,i}$ and optimum value of θ. Similarly, tables 4 and 5 give results obtained considering the combined effect of the first 4-5 beam modes (with minimum length of 0.005 m).

Figures 7 through 10 show placement of sensor-actuator pairs and the curve of the cost function for the fittest individual of the population considering the effect of the first four beam modes separately. Figures 11 and 12 illustrate the development of target function taking into account the combined effect of the first four and of the first five natural modes respectively. Moreover, in this last case the number of sensor-actuator pairs considered were 4 and 5 respectively.

Conclusions

To control vibration of a composite beam the authors determined the optimum placement and size of piezoelectric sensor and actuator pairs, and fiber orientation of one of the layers of the laminated composite beam. The finite element method was used to discretize the Reissner-Mindlin model of a multilayered plate featuring piezoelectric layers acting as sensors or actuators.

Comparison of simulations with experimental results available from the literature prove the effectiveness of the model based on plates incorporating piezoelectric layers. Results obtained highlight the importance of taking into account damping of piezoelectrics and of the adhesive layer in connection with dynamic analysis of a structure.

The use of an optimization model required the development of a procedure for automatic mesh generation able to meet mechanical and electrical boundary conditions. The optimization problem was solved by adopting a target function which includes damping in the form of the product of damping ratio by natural frequency for a given number of modes. Finally, the method outlined herein may be extended by introducing factors c_j from (29) allowing greater emphasis to be placed only on some modes of the structure without suppressing others.

Acknowledgements

The authors wish to thank Dr E. Carrera for his advice during development of the multilayered plate model.

References

[1] Crawley, E., de Luis, J., 'Use of Piezoelectric Actuators as Elements of Intelligent Structures', AIAA Journal, Vol.25(10), 1987, pp. 1373-1385.

[2] Bailey, T., Hubbard, J.E., 'Distributed Piezoelectric Polymer Active Vibration Control of a Cantilever Beam', Journal of Guidance, Control and Dynamics, Vol.8(5), 1985, pp. 605-611.

[3] Lindberg, R.E., 'Actuator Placement Considerations for the Control of Large Space Structures', Journal of Guidance, Control and Dynamics, Vol. 15(1), 1992, pp. 49-57.

[4] Batra, R.C., Lian, X.Q., Yang, J.S., 'Shape Control of Vibrating Simply Supported Rectangular Plates', AIAA Journal, Vol.34(1), 1996, pp. 116-122.

[5] Devasia, S., Meressi, T., Paden, B., Bayo, E., 'Piezoelectric Actuator Design for Vibration Suppression: Placement and Sizing', Journal of Guidance, Control and Dynamics, Vol.16(5), 1993, pp. 859-864.

[6] Goldberg, G.E., 'Genetic Algorithms in Search, Optimisation and Machine Learning', 1989.

[7] Onoda, J., Hanawa, Y., 'Actuator Placement Optimization by Genetic and Improved Simulated

Annealing Algorithms',AIAA Journal, Vol.31(6), 1992, pp. 1167-1169.

[8] Gaudenzi, P., Fantini, E., Koumousis, V., Gantes, C.,'Optimization of Lengths and Position of PZT Actuators for the Active Control of a Beam by Means of Genetic Algorithms, 7th ICAS, September 1996,pp. 400-411.

[9] Carrera, E., 'An Improved Reissner-Mindlin-Type Model for the Electromechanical Analysis of Multilayered Plates Including Piezo-Layers', in preparation, Department of Aeronautical and Space Engineering, Politecnico di Torino, 1998.

[10] Lin, D.X., Ni, R.G., Adams, R.D., 'Prediction and Measurement of the Vibrational Damping Parameters of Carbon and Glass Fibre-Reinforced Plastics Plates', Journal of Composite Materials, Vol.18, March 1994, pp. 132-152.

[11] Bathe, K.J., 'Finite Element Procedures in Engineering Analysis', Prentice-Hall, Englewood Cliffs, NJ, 1982.

[12] Hwang, W.S., Park, H.C., 'Finite Element Modeling of Piezoelectric Sensors and Actuators', AIAA Journal, Vol.31(5), 1993, pp. 930-937.

[13] Tzou, H.S., Tseng, C.I., 'Distributed Vibration Control and Identification of Coupled Elastic/Piezoelectric Systems: Finite Element Formulation and Applications', Mechanical Systems and Signal Processing, Vol.5(3), 1991, pp. 215-231.

[14] Kang, Y.K., Park, H.C., Hwang, W., Han, K.S., 'Prediction and Measurement of Modal Damping of Laminated Composite Beams with Piezoceramic Sensor/Actuator', Journal of Intelligent Material Systems ans Structures, Vol.7, January 1996, pp. 25-32.

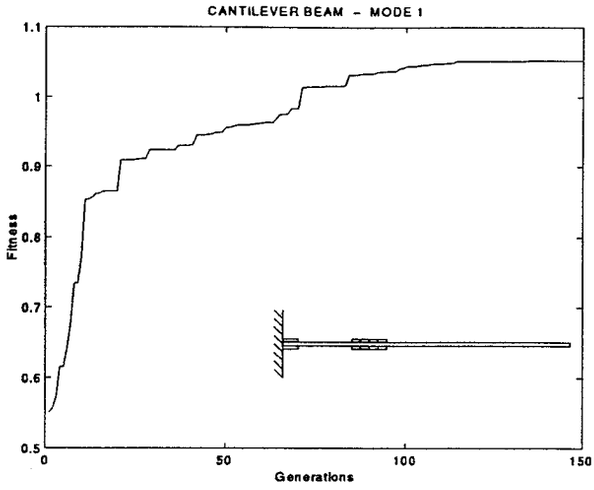

Figure 7: Objective function for mode no.1

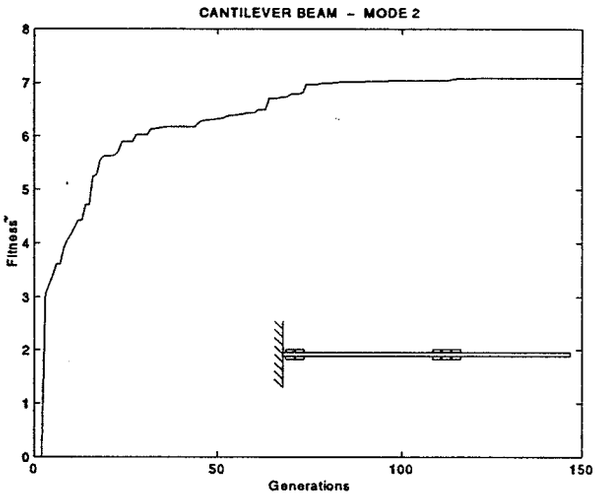

Figure 8: Objective function for mode no.2

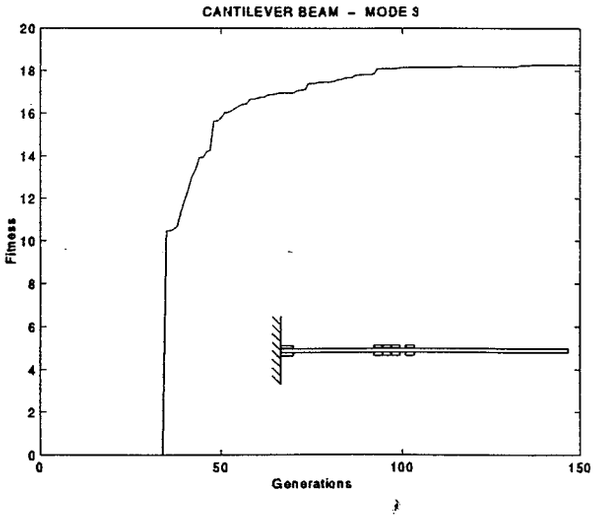

Figure 9: Objective function for mode no.3

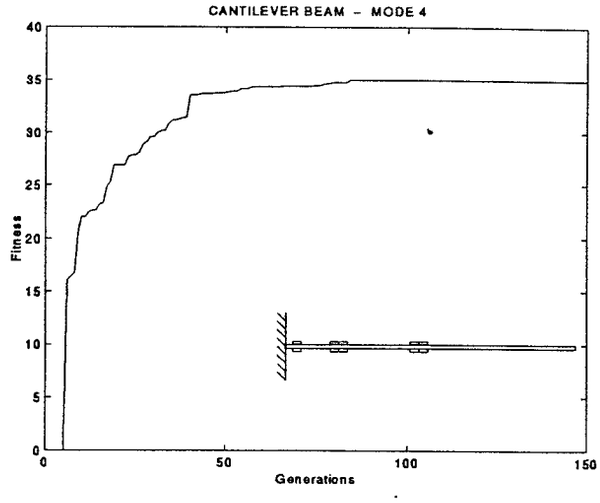

Figure 10: Objective function for mode no.4

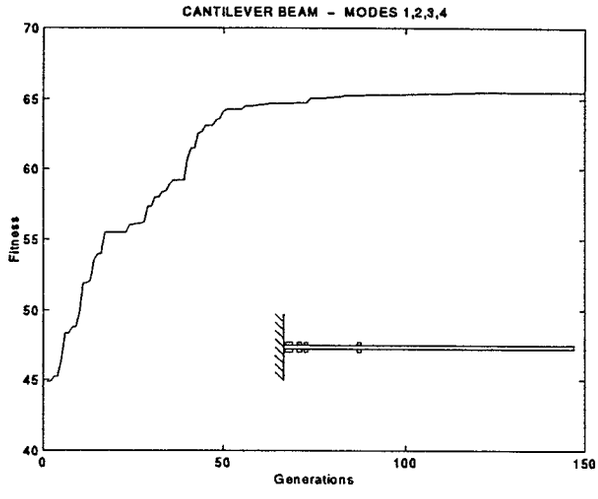

Figure 11: Objective function for mode no.1 to 4

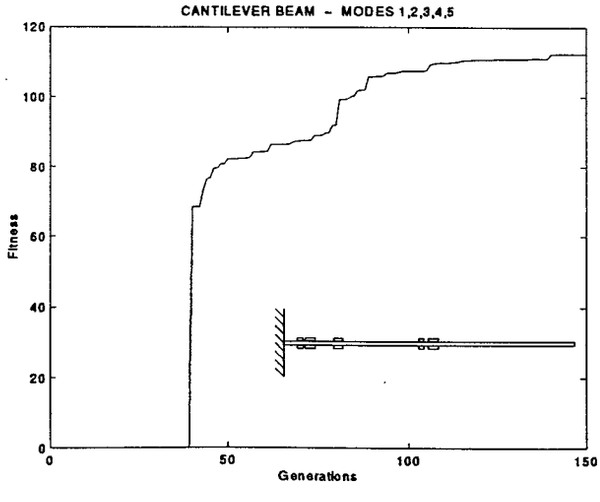

Figure 12: Objective function for mode no.1 to 5

Mode no.	$p_{x,1}$	$p_{x,2}$	$p_{x,3}$	$p_{x,4}$	$p_{x,5}$
1	0.0085	0.1017	0.1117	0.1217	0.1322
2	0.0079	0.0181	0.1765	0.1865	0.1965
3	0.0072	0.1096	0.1199	0.1305	0.1459
4	0.0129	0.0742	0.0847	0.1443	0.1547

Table 2: Centerline position [m] of each piezoelectric patch from the clamped end - results for each individual mode

Mode no.	$l_{x,1}$	$l_{x,2}$	$l_{x,3}$	$l_{x,4}$	$l_{x,5}$	θ
1	0.0170	0.0100	0.0100	0.0100	0.0100	22^o
2	0.0102	0.0100	0.0100	0.0100	0.0100	19^o
3	0.0135	0.0101	0.0100	0.0101	0.0100	22^o
4	0.0100	0.0100	0.0100	0.0100	0.0100	20^o

Table 3: Length [m] of each piezoelectric patch and optimal value of θ [deg] - results for each individual mode

Mode no.	$p_{x,1}$	$p_{x,2}$	$p_{x,3}$	$p_{x,4}$	$p_{x,5}$
1,2,3,4	0.0050	0.0181	0.0251	0.0874	-
1,2,3,4,5	0.0179	0.0289	0.0631	0.1541	0.1657

Table 4: Centerline position [m] of each piezoelectric patch from the clamped end - combined effect of first 4/5 modes

Mode no.	$l_{x,1}$	$l_{x,2}$	$l_{x,3}$	$l_{x,4}$	$l_{x,5}$	θ
1,2,3,4	0.0086	0.0050	0.0050	0.0050	-	22^o
1,2,3,4,5	0.0058	0.0113	0.0099	0.0056	0.0109	19^o

Table 5: Length [m] of each piezoelectric patch and optimal value of θ [deg] - combined effect of first 4/5 modes